AIP | Applied Physics Letters

Exploiting phase separation in monolithic La0.6Ca0.4MnO3 devices

L. Granja, L. E. Hueso, P. Levy, and N. D. Mathur

Citation: Appl. Phys. Lett. **103**, 062404 (2013); doi: 10.1063/1.4818314
View online: http://dx.doi.org/10.1063/1.4818314
View Table of Contents: http://apl.aip.org/resource/1/APPLAB/v103/i6
Published by the AIP Publishing LLC.

Exploiting phase separation in monolithic $La_{0.6}Ca_{0.4}MnO_3$ devices

L. Granja,[1,2] L. E. Hueso,[3,4,5] P. Levy,[1,2] and N. D. Mathur[3,a)]
[1]*Departamento de Materia Condensada, Gerencia de Investigación y Aplicaciones, Comisión Nacional de Energía Atómica, General Paz 1499 (1650), San Martín, Buenos Aires, Argentina*
[2]*Consejo Nacional de Investigaciones Científicas y Técnicas, Rivadavia 1917 (C1033AAJ), Ciudad Autónoma de Buenos Aires, Argentina*
[3]*Department of Materials Science, University of Cambridge, 27 Charles Babbage Road, Cambridge CB3 0FS, United Kingdom*
[4]*CIC nanoGUNE Consolider, Tolosa Hiribidea 76, E-20018, Donostia-San Sebastian, Spain*
[5]*IKERBASQUE, Basque Foundation for Science, E-48011 Bilbao, Spain*

(Received 29 March 2013; accepted 26 July 2013; published online 9 August 2013)

Devices based on mesas were fabricated from thin films of magnetically phase-separated $La_{0.6}Ca_{0.4}MnO_3$. Low-field magnetoresistance arises because the volume fraction of the ferromagnetic metallic phase is large enough for percolation but small enough to permit magnetic decoupling between each mesa and the underlying track. Magnetic domain walls in the antiparallel mesa-track configuration possess a giant resistance-area product of $(3–7) \times 10^{-8}\,\Omega m^2$. This figure represents an 11 order-of-magnitude improvement with respect to the figure for cobalt. © *2013 AIP Publishing LLC*. [http://dx.doi.org/10.1063/1.4818314]

Low-field magnetoresistance (LFMR) may be achieved by controlling the relative magnetic alignment of ferromagnetic electrodes using an applied magnetic field. It has been exploited in disc-drive read heads using electrodes fabricated from traditional ferromagnetic metallic (FMM) materials where the spin polarization is ~40%,[1] and it has been explored in various devices using electrodes fabricated from ferromagnetic manganites where the spin polarization can approach 100%.[2] In these manganite devices, the high-resistance antiparallel configuration has been hitherto achieved by magnetically decoupling the two electrodes via tunnel barriers,[3–5] grain boundaries,[6–8] nanoconstrictions[9,10] and phase-separated manganite layers.[11–13] Here we investigate whether magnetically decoupled electrodes can be obtained in a device possessing no discontinuities in structure or chemistry.

In bulk, the FMM manganites $La_{0.70}Ca_{0.30}MnO_3$ (LCMO30) and $La_{0.60}Ca_{0.40}MnO_3$ (LCMO40) show nominally no phase separation well below Curie temperature $T_C \sim 260\,K$.[14] Epitaxial films of LCMO30 behave similarly, but epitaxial films of LCMO40 are magnetically phase separated at low temperatures such that a paramagnetic insulator (PMI) phase coexists with an FMM phase that occupies ~40% of the sample volume.[12,15] Here we exploit this phase separation in LCMO40 films to achieve LFMR in current-perpendicular-to-the-plane (CPP) mesa devices with no structural/chemical discontinuities.[3–13] A control experiment with an LCMO30 mesa device was used to confirm the need for phase separation, and a previously published[12] control experiment with an unpatterned LCMO40 film was used to confirm the need for mesas.

As described in Ref. 15, we used pulsed laser deposition to grow 80 nm-thick films of LCMO30 and LCMO40 on $NdGaO_3$ (001) substrates, and we protected the films for subsequent processing using an Ag cap, deposited *in situ* by pulsed laser deposition under vacuum. X-ray diffraction confirmed the epitaxy and crystalline quality of our manganite films. Square mesas of side 5–18 μm were defined with electrical contacts (left inset of Fig. 1) using optical lithography, Ar-ion milling, sputtered Ag, and sputtered SiO_2, in a process described elsewhere.[4,12,13] Four-terminal CPP resistance measurements were performed in a closed-cycle He cryostat and a Quantum Design Physical Property Measurement System (PPMS), using measurement currents of 1 μA and 0.1 μA, respectively. At various temperatures, data were collected as a function of magnetic field applied parallel to the magnetic easy axis, i.e., along the orthorhombic [100] film direction.[12]

Before investigating LFMR, we confirmed that our mesa devices are magnetically phase separated by studying high-field magnetoresistace (HFMR), as this has been used to reveal phase separation in manganites with other geometries[13] and compositions.[16] For LCMO40 mesa devices at 25 K, the initial application of a $\mu_0 H \sim 4\,T$ magnetic field produced a ~90% fall in resistance-area product (RA) and further field cycling yielded reproducible high-field hysteresis (Fig. 1). By contrast, a control mesa device fabricated from LCMO30 showed a much smaller 25 K HFMR of around $-5\%\ T^{-1}$ (right inset of Fig. 1), as expected for single-phase colossal magnetoresistance (CMR) materials when a large magnetic field aligns Mn core spins.[14] The very large high-field changes in our LCMO40 mesa devices arise due to changes in FMM volume fraction,[13,16] thus confirming phase separation. Above the reversibility field of $\mu_0 H \sim 5\,T$, the HFMR of around $-7\%\ T^{-1}$ is typical for single-phase CMR materials below T_C,[13] as discussed above.

LCMO40 devices comprising variable-size mesas showed LFMR ~ 5% at 25 K (Fig. 2). The phase separation is required given that an LCMO30 mesa device showed no LFMR (right inset of Fig. 2), and the mesas are required given that an unpatterned LCMO40 film has been shown[12] to display a qualitatively different LFMR (sharp ~2% drops in resistance near the coercive field due to CMR). LFMR

a)Author to whom correspondence should be addressed. Electronic mail: ndm12@cam.ac.uk

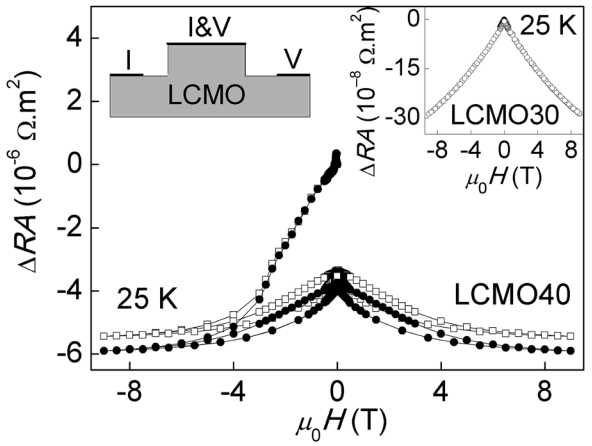

FIG. 1. For two of the mesa devices described in Fig. 2 [5 μm × 5 μm (solid circles), 6 μm × 6 μm (open squares)], we show changes in high-field CPP resistance-area product $\Delta RA = RA(H) - RA(0)$ after zero-field cooling to 25 K. Left inset: device schematic for $La_{1-x}Ca_xMnO_3$ (LCMO), not to scale, showing contact pads (thick lines) for voltage V and current I connections. Right inset: equivalent data for the 5 μm × 5 μm mesa when LCMO40 is replaced by LCMO30.

magnitude depends strongly on track and contact resistance, so there is plenty of scope for optimizing our proof-of-principle devices based on the values of ΔRA that we report here.

For each mesa device, the sharp increases in resistance at $\mu_0 H \sim \pm 25$ mT (Fig. 2) occur very near the coercive field of unpatterned films[12] and therefore arise due to magnetization reversal in the track. The high-resistance state associated with the antiparallel mesa-track configuration is achieved because track reversal does not force mesa reversal, as magnetic domain walls (dotted lines in Fig. 3(a)) need only form across FMM regions rather than across each entire mesa, thus reducing magnetic domain-wall energy.

Having reached the high-resistance state on a major loop, further increasing the magnitude of the field yielded a subsequent decrease in resistance over a relatively wide range of fields prior to loop closure (Fig. 2). This indicates that the parallel mesa-track configuration (Fig. 3(b)) is reached via gradual magnetization reversal in the mesa. This gradual switching is probably due to the rough mesa edges

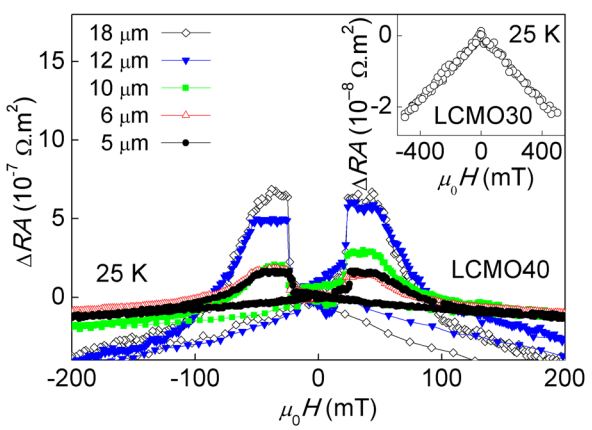

FIG. 2. Low-field changes in CPP resistance-area product $\Delta RA = RA(H) - RA(0)$, for devices comprising square mesas of side lengths 5–18 μm. These mesas were defined in an 80 nm film of LCMO40 and measured in $\mu_0 H = \pm 0.4$ T after zero-field cooling to 25 K. Right inset: equivalent data for the 5 μm × 5 μm mesa when LCMO40 is replaced by LCMO30.

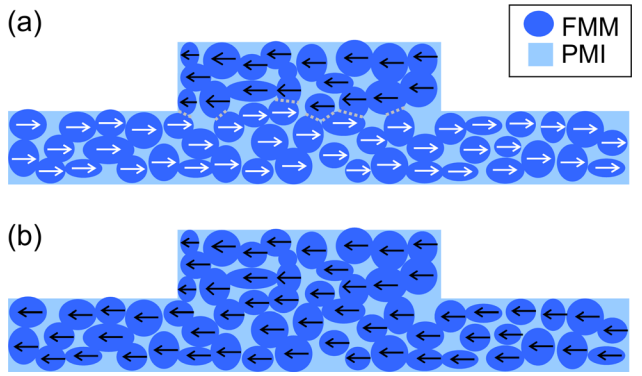

FIG. 3. Schematic (not to scale) of an LCMO40 mesa device in (a) antiparallel and (b) parallel mesa-track configurations. For each FMM island in the PMI background, magnetization direction is indicated by arrow direction and colour. Domain walls (dotted lines) in FMM regions do not span the entire mesa, which is thus weakly coupled to the underlying track.

exerting variable degrees of pinning on poorly connected FMM regions, but inhomogeneity associated with strain relaxation at edges[17] could also play a role.

LFMR falls with increasing temperature and is lost near T_C, which lies just above 200 K (Fig. 4). However, the LFMR at 25 K is highly reproducible after an excursion above T_C (Fig. 5). This is attributed to fixed patterns of strain, and thus fixed patterns of phase separation, as seen for an LCMO40 film using conducting-tip atomic force microscopy (CT-AFM) and magnetic force microscopy (MFM).[12] Of particular interest here is our observation that the parallel and antiparallel mesa-track configurations may be achieved at zero field by executing a minor loop that reverses track

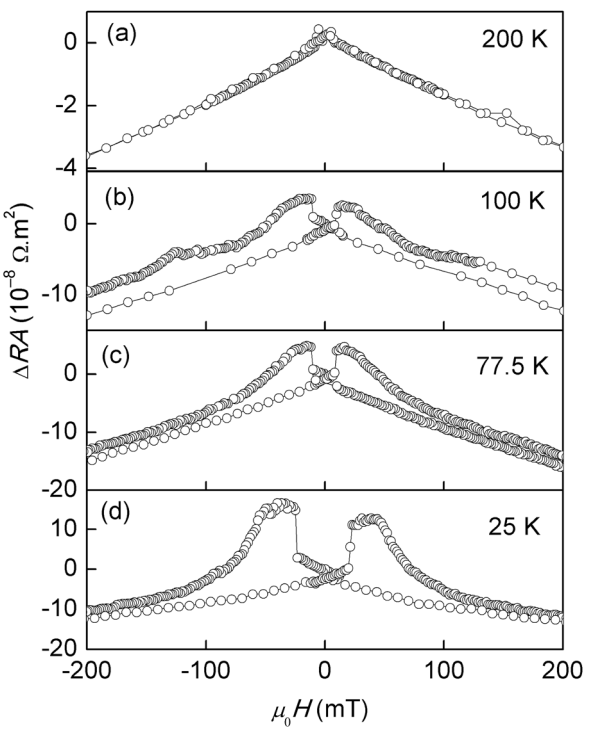

FIG. 4. For the 6 μm × 6 μm mesa device described in Fig. 2, we show low-field changes in CPP resistance-area product $\Delta RA = RA(H) - RA(0)$ at selected temperatures, after zero-field cooling from 300 K to the measurement temperature. Data measured in $\mu_0 H = \pm 0.4$ T.

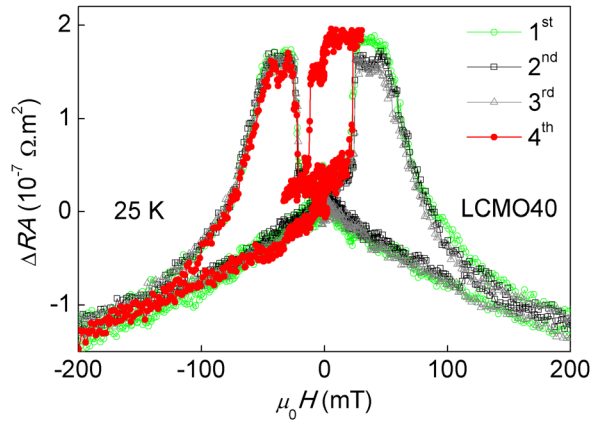

FIG. 5. For the 5 μm × 5 μm LCMO40 mesa device described in Figure 2, we show low-field changes in CPP resistance-area product $\Delta RA = RA(H) - RA(0)$. Each of the three major loops was measured in the order shown, by first zero-field cooling to 25 K, and then sweeping the applied field in $\mu_0 H = \pm 0.4$ T. After zero-field cooling to 25 K for a fourth time, we measured part of a major loop and then measured a minor loop in $\mu_0 H = \pm 35$ mT.

magnetization but not mesa magnetization (Fig. 5). This confirms non-volatile resistance switching.

Devices with sufficiently large mesas showed a larger jump in resistance-area product *RA* when switching between parallel and antiparallel configurations (Fig. 2). This is likely due to inhomogenous current flow[18,19] and/or an effective reduction in mesa perimeter due to the ion-milling damage that is responsible for the roughness described above. However, mesas smaller than 10 μm × 10 μm all show $\Delta RA = RA(H) - RA(0) = (1.6 \pm 0.3) \times 10^{-7}\,\Omega m^2$ at 25 K. Given that FMM islands occupy an areal fraction of 20%–42% in similar films of LCMO40,[12] the change in resistance-area product for domain walls in the FMM phase alone may be estimated to lie in the range $(3–7) \times 10^{-8}\,\Omega m^2$. This domain-wall resistance is several orders of magnitude larger than the large values obtained using mesas fabricated from trilayers ($10^{-12}\,\Omega m^2$ for LCMO30/LCMO40/LCMO30 (Refs. 12 and 13) and $10^{-10}\,\Omega m^2$ for LCMO30/LCMO41/LCMO30). We suggest that the dramatic increase observed here could be explained if our domain walls are more constrained[20] than those in CPP trilayers.[12,13] By comparison, the $10^{-19}\,\Omega m^2$ resistance-area product of domains walls in cobalt[21] is much smaller.

In summary, we have studied mesa devices fabricated from thin films of LCMO40. We have confirmed phase separation by observing HFMR due to variations in FMM phase fraction,[13,16] and we have demonstrated LFMR due to the reproducible creation of magnetic domain walls between each mesa and the underlying track. These domain walls lie in FMM pathways[12] that provide weak magnetic links, and therefore structural[6–10]/chemical[3–5,11–13] discontinuities are not required in order to achieve an antiparallel mesa-track configuration. The giant resistance-area product of $(1.6 \pm 0.3) \times 10^{-7}\,\Omega m^2$ at 25 K evidences a giant domain-wall resistance-area product of $(3–7) \times 10^{-8}\,\Omega m^2$, indicating that the domain walls here are significantly constrained. These self-organized domain walls represent a third way[22] of nanopatterning, which differs from traditional top-down and bottom-up fabrication. Taken more generally, our findings demonstrate the value of exploiting phase separation in manganite devices.

We thank L. Fraigi *et al.* at INTI for technical support. This work was funded by the EU Alban program (L.G.), the EU Marie Curie scheme (L.E.H.), and the U.K. EPSRC.

[1]R. Meservey and P. M. Tedrow, Phys. Rep. **238**, 173 (1994).
[2]J.-H. Park, E. Vescovo, H.-J. Kim, C. Kwon, R. Ramesh, and T. Venkatesan, Nature **392**, 794 (1998).
[3]J. Z. Sun, W. J. Gallagher, P. R. Duncombe, L. Krusin-Elbaum, R. A. Altman, A. Gupta, Y. Lu, G. Q. Gong, and G. Xiao, Appl. Phys. Lett. **69**, 3266 (1996).
[4]M.-H. Jo, N. D. Mathur, N. K. Todd, and M. G. Blamire, Phys. Rev. B **61**, R14905 (2000).
[5]M. Bowen, M. Bibes, A. Barthélémy, J.-P. Contour, A. Anane, Y. Lemaître, and A. Fert, Appl. Phys. Lett. **82**, 233 (2003).
[6]H. Y. Hwang, S-W. Cheong, N. P. Ong, and B. Batlogg, Phys. Rev. Lett. **77**, 2041 (1996).
[7]A. Gupta, G. Q. Gong, G. Xiao, P. R. Duncombe, P. Lecoeur, P. Trouilloud, Y. Y. Wang, V. P. Dravid, and J. Z. Sun, Phys. Rev. B **54**, R15629 (1996).
[8]N. D. Mathur, G. Burnell, S. P. Isaac, T. J. Jackson, B. S. Teo, J. L. MacManus-Driscoll, L. F. Cohen, J. E. Evetts, and M. G. Blamire, Nature (London) **387**, 266 (1997).
[9]J. Wolfman, A. M. Haghiri-Gosnet, B. Raveau, C. Vieu, E. Cambril, A. Cornette, and H. Launois, J. Appl. Phys. **89**, 6955 (2001).
[10]T. Arnal, A. V. Khvalkovskii, M. Bibes, B. Mercey, P. Lecoeur, and A. M. Haghiri-Gosnet, Phys. Rev. B **75**, 220409(R) (2007).
[11]L. E. Hueso, L. Granja, P. Levy, and N. D. Mathur, J. Appl. Phys. **100**, 023903 (2006).
[12]C. Israel, L. Granja, T. M. Chuang, L. E. Hueso, D. Sánchez, J. L. Prieto, P. Levy, A. de Lozanne, and N. D. Mathur, Phys. Rev. B **78**, 054409 (2008).
[13]L. Granja, L. E. Hueso, J. L. Prieto, P. Levy, and N. D. Mathur, Appl. Phys. Lett. **97**, 253501 (2010).
[14]S.-W. Cheong and H. Y. Hwang, in *Colossal Magnetoresistive Oxides*, edited by Y. Tokura (Gordon and Breach, Amsterdam, 2000).
[15]D. Sánchez, L. E. Hueso, L. Granja, P. Levy, and N. D. Mathur, Appl. Phys. Lett. **89**, 142509 (2006).
[16]P. Levy, F. Parisi, L. Granja, E. Indelicato, and G. Polla, Phys. Rev. Lett. **89**, 137001 (2002).
[17]Y.-A. Soh, P. G. Evans, Z. Cai, B. Lai, C.-Y. Kim, G. Aeppli, N. D. Mathur, M. G. Blamire, and E. D. Isaacs, J. Appl. Phys. **91**, 7742 (2002).
[18]R. J. M. van de Veerdonk, J. Nowak, R. Meservey, J. S. Moodera, and W. J. M. de Jorge, Appl. Phys. Lett. **71**, 2839 (1997).
[19]J. S. Moodera, L. R. Kinder, J. Nowak, P. LeClair, and R. Meservey, Appl. Phys. Lett. **69**, 708 (1996).
[20]P. Bruno, Phys. Rev. Lett. **83**, 2425 (1999).
[21]U. Rüdiger, J. Yu, L. Thomas, S. S. P. Parkin, and A. D. Kent, Phys. Rev. B **59**, 11914 (1999).
[22]N. Mathur and P. Littlewood, Nature Mater. **3**, 207 (2004).